HHS Public Access

Author manuscript

Vision Res. Author manuscript; available in PMC 2018 July 01.

Published in final edited form as:

Vision Res. 2017 July ; 136: 1–14. doi:10.1016/j.visres.2017.04.008.

Paradoxical perception of object identity in visual motion

Aleksandra Zharikova[1], **Sergei Gepshtein**[2], and **Cees van Leeuwen**[1,3]

[1]Laboratory for Perceptual Dynamics, University of Leuven, Belgium

[2]Center for Neurobiology of Vision, Salk Institute for Biological Studies, USA

[3]Center for Cognitive Science, TU Kaiserslautern, Germany

Abstract

In the course of perceptual organization, incomplete optical stimulation can evoke the experience of complete objects with distinct perceptual identities. According to a well-known principle of perceptual organization, stimulus parts separated by shorter spatial distances are more likely to appear as parts of the same perceptual identity. Whereas this principle of proximity has been confirmed in many studies of perceptual grouping in static displays, we show that it does not generalize to perception of object identity in dynamic displays, where the parts are separated by spatial and temporal distances. We use ambiguous displays which contain multiple moving parts and which can be perceived two ways: as two large objects that gradually change their size or as multiple smaller objects that rotate independent of one another. Grouping over long and short distances corresponds to the perception of the respectively large and small objects. We find that grouping over long distances is often preferred to grouping over short distances, against predictions of the proximity principle. Even though these effects are observed at high luminance contrast, we show that they are consistent with results obtained at the threshold of luminance contrast, in agreement with predictions of a theory of efficient motion measurement. This is evidence that the perception of object identity can be explained by a principle of neural economy rather than by the empirical principle of proximity.

Keywords

perceptual organization; grouping; perceptual identity; apparent motion; contrast sensitivity; neural economy

Introduction

In dynamic scenes, parts of optical stimuli presented at different locations and different instants can “group” across space and time, i.e., appear to belong to the same object. This perceptual grouping gives rise to the experience of moving objects. How do visual systems derive stable object identities while the corresponding parts of stimulations are separated in space and time? This question was enunciated by Gestalt psychologists as the problem of “phenomenal identity” (Wertheimer, 1923; Ternus, 1926) and it instigated numerous studies

Corresponding author: Aleksandra Zharikova, Faculty of Psychology and Educational sciences, KULeuven, Tiensestraat 102, Box 3711, 3000 Leuven, Belgium, Tel +32 16 32 57 27, aleksandra.zharikova@kuleuven.be.

(Jones & Bruner, 1954; Bower, 1967; Kellman & Spelke, 1983; Hochberg, 1987; Dawson, 1991; Kahneman, Treisman, & Gibbs, 1992; Chun, 1997; Gepshtein & Kubovy, 2000; Moore, Stephens, & Hein, 2010).

Several authors proposed that the experience of object identity was mediated by perceptual grouping according to the principle of proximity (Ternus, 1926; Kramer & Yantis, 1997; He & Ooi, 1999). According to this notion, stimulus parts separated by a shorter distance are more likely to group together. The principle was found to hold in many static visual displays (Oyama, 1961; Hochberg, 1974; Kubovy & Wagemans, 1995; Pomerantz & Portillo, 2011). It was expected to hold also in dynamic displays, where stimulus parts are separated by spatial and temporal distances. For example, the "Ternus display" (Figure 1A) consists of two pairs of dots: marked "1" and "2" in the first frame t_1 and "3" and "4" in the second frame t_2. This display can be perceived in two ways. Spatial grouping of the concurrent dots {1, 2} and {3, 4} with consequent matching of the groups {1, 2} and {3, 4} leads to the perception of a single moving object: a group of dots ("group motion"). Alternatively, spatiotemporal grouping of dots {1, 4} and {2, 3} leads to the perception of two distinct moving objects ("element motion"). Decreasing spatial distances between the dots within frames makes group motion more likely, and decreasing temporal distance between the dots (i.e., decreasing temporal intervals between the frames) makes element motion more likely (Ternus, 1926; Petersik & Pantle, 1979; Kramer & Yantis, 1997).

Yet the results obtained with such simple dynamic displays do not generalize to more complex dynamic stimuli. For example, consider the stimulus called "motion lattice" (Gepshtein & Kubovy, 2000). Figure 1B is a schematic representation of two frames of a motion lattice seen through a circular aperture. In the first frame, dots appear in the even rows of the lattice; in the second frame they appear in the odd rows. Alternation of frames gives rise to the perception of upward or downward motion. For example, downward-right motion is seen when the dots are grouped between frames along the arrow drawn between dots 2 to 4, and downward-left motion is seen along the arrow between dots 2 to 3. Both are element motions. Their directions differ from the vertical "group motion," which is seen when the dots group within rows and then the rows are grouped between frames. Perception of element motion or group motion depends on spatial distances within frames and spatiotemporal distances between frames.

Further studies using motion lattices suggested that perception of dynamic displays is not always consistent with the proximity principle. Gepshtein & Kubovy (2007) found that at small spatiotemporal scales increasing the spatiotemporal distances between dots makes their grouping more rather than less likely. These results were consistent with a characteristic of visibility of periodic visual patterns (Gepshtein & Kubovy, 2007) and with an analysis of efficiency of visual measurement across the full range of visible spatiotemporal scales (Gepshtein & Kubovy, 2007; Gepshtein, Tyukin, & Kubovy, 2007; Jurica, Gepshtein, Tyukin, & van Leeuwen, 2013).

In the motion lattices just described, perception of objects with distinct identities arises by virtue of grouping of individual dots between frames. In a different type of motion lattice introduced by Gepshtein & Kubovy (2000), two distinct object identities could be perceived:

rows of dots (“moving objects”) vs. individual dots (“moving dots”). Perception of moving objects corresponded to the grouping of dots within frames and matching of the resulting groups between frames. Perception of moving dots corresponded to a lower-scale grouping between frames. The perception of moving objects could be disrupted by changing dot distances between the frames, indicating that perception of object identity can be controlled by a balance of spatiotemporal distances between display elements, just as the perception of apparent motion.

Here we use different displays, introduced by Anstis & Kim (2011), where groupings with distinct identities can arise *within* frames, but where the perception of identity can be enhanced or disrupted by grouping *between* frames. The resulting objects have different shapes, which makes the alternative perceptual identities particularly compelling. The displays consist of multiple rotating dot pairs, which we call “dipoles.” The dipoles are arranged on an invisible circle as shown in Figure 1C. Motion is perceived when the dots group between frames, i.e., across distance m. (For example, consider the grouping of dots 1 and 3 or the grouping of dots 2 and 4 in Figure 1C.) Perceived object identities depend on whether the dots group within dipoles (across the spatial distance Δw within frames) leading to the perception of multiple rotating dot pairs (top of the middle panel in Figure 1C; see Movie 1), or the dots group between dipoles (across the spatial distance Δb within frames) leading to the perception of two pulsating circles (bottom of the middle panel in Figure 1C; Movie 2). Since the distance m does not co-vary with the distances Δw and Δb, we can keep m constant while separately varying Δw and Δb. This way, the perception of identity can change while dot trajectories remain the same.

We vary distances within and between the dipoles and measure observer preferences for perception of rotating “dipoles” vs. pulsating “circles” We find that the effect of proximity on perception of object identity is paradoxical in the following sense. In many cases, increasing the spatial and temporal distances between the dots makes their grouping more likely (rather than less likely, as expected from the Gestalt principle of proximity). In particular, pulsating circles are perceived even when the spatial distances between the dipoles are significantly longer than the spatial distances within the dipoles (see Supplementary Animation). We show, however, that the results that appear paradoxical from the Gestalt perspective are coherent from another perspective. They are consistent with the predictions derived from a basic characteristic of visibility of periodic spatiotemporal patterns.

Experiment 1: Object identity as a function of spatial distance

Before we turn to effects of *spatiotemporal* proximity, we study a simpler case of how object identity is affected by *spatial* proximity between elements of a dynamic display.

Methods

Stimuli—Several dot pairs (“dipoles”) appeared on an invisible circle of radius 3 degrees of visual angle (deg) with a white fixation dot in the center. The number of dot pairs was one of the manipulated variables, as well as distance between the dot pairs Δb. The dots had a diameter of 0.4 deg and luminance of 128.6 cd/cm^2. They appeared on a uniform gray

background with luminance of 33.5 cd/cm^2. The display consisted of 8 frames presented in a continuous cycle so that the first frame was presented after the eighth one. Between successive frames the dots were displaced by $2\pi/16$ on a circle of diameter Δw so that the dipoles appeared rotating around their centers. The inter-frame interval was 0 ms; each frame was presented for a time period equal to Δt.

Apparatus—The experiments were controlled by PsychoPy software (Peirce, 2007) on a Dell Precision T3500 workstation using an LCD monitor (Dell U2410) with a spatial resolution of 1920×1200 and a refresh rate of 60 Hz. A head-and-chin-rest was used to stabilize the viewing conditions. Observers viewed the stimuli in a dimly lit room at a distance of 80 cm from the monitor.

Procedure—Stimuli were presented for 510 ms. In a series of pilot experiments where the stimulus was presented for 510, 1360, and 2500 s confirmed that observers were able to see both “dipoles” and “circles” across the full range of conditions tested in the subsequent experiments. Observers were instructed to fixate at the central dot while watching the stimulus. They reported whether they perceived dipoles or circles by pressing one of two keyboard keys. Trials were separated by a blank interval of 500 ms. Before each session, observers performed 8–10 practice trials; they made a verbal response following each stimulus and then pressed a response key, corrected by the experimenter if the key response failed to match the verbal response. During the practice trials, we ascertained that all observers were able to see both percepts of “dipoles” and “circles”. We varied within-dipole distance Δw and between-dipole distance Δb, keeping Δt constant at 170 ms. We used five distances Δw (0.15, 0.25, 0.38, 0.64 and 1.28 deg). The trials were presented in blocks of 100, in which both Δw and Δt were fixed, while Δb was controlled by an adaptive method: the PSI procedure (Kontsevich & Tyler, 1999). Distance Δb was varied by changing the number of dipoles. Distance Δb was varied by changing the number of dipoles. The smallest and largest numbers of dipoles were three and fifty. Distance Δb was varied within the range between $0.5\Delta w$ and $30\Delta w$. Four naïve observers took part in the experiment. All observers had normal or corrected-to-normal vision and signed informed consent before participating. The experiments were carried out in accordance with the Code of Ethics of the World Medical Association (Declaration of Helsinki). The study was approved by the ethics review board of the University of Leuven.

Results

Grouping of dots within dot pairs over distance Δw corresponds to the perception of rotating dipoles (“dipoles”) and grouping of dots between dot pairs over distance Δb corresponds to the perception of pulsating circles (“circles”). We varied distances Δw and Δb and measured preferences for two percepts, dipoles vs. circles as a function of distance ratio: $R = \Delta b/\Delta w$.

We identified the transition ratios, R^*, at which the alternative groupings were equally likely. For distance ratios greater than transition ratios R^*, the display was perceived as “dipoles”. For distance ratios smaller than transition ratios R^*, the display was perceived as “circles.”

To obtain the magnitude of R^* for every observer, we computed the log-odds of responses “circle” and “dipoles” for every distance ratio R:

$$L=\log(N_c/N_d),$$

where N_c and N_d are the numbers of responses “circles” and “dipoles”, respectively; log is a logarithm of base 10. (The arbitrary value of 1/6 is added to the numerator and denominator in order to avoid division by zero; Tukey, 1977). In Figure 2A, the log-odds are plotted as a function of distance ratio R and fitted with the logistic function. Transition ratios R^* are the magnitudes of R at which the log-odds are zero. Figure 2B is a plot of transition ratios as a function of distance Δw for four observers (the averaged data are presented in supplemental Figures S1–S4). At small distances Δw the transition ratios are larger than unity, in violation of the Gestalt principle of proximity. Note that individual data vary between observers. As we will show further in Experiment 4, individual variability of transition ratios could be predicted from individual variability in visual sensitivity to sinusoidal luminance patterns, which is known significantly vary between subjects (Ginsburg, Evans, Cannon, Owsley, & Mulvanny, 1984; Evans & Ginsburg, 1985; Peterzell & Teller, 1996; Peterzell, Werner, & Kaplan, 1995).

In Experiment 1, two variables were manipulated jointly: the inter-dipole distance Δb and the number of dipoles. The transition point between the percepts of “dipoles” vs. “circles” could depend on the number of the dipoles, rather than on the distance ratios $R^* = \Delta b/\Delta w$. If that were the case, the number of dipoles at the transition point would be constant over distance Δw. Distance Δb at the transition point would also be constant over distance Δw, because Δb changed together with the number of the dipoles. Figures 3 and 4 provide an indication that, at points of transition, both number of dipoles and distance Δb depended on within-dipole distance Δw, suggesting that it was not the number of the dipoles that controlled transition between the perception of “dipoles” and “circles.”

In Figure 3, results of Experiment 1 are plotted in terms of the number of dipoles. Figure 3A is a plot of the log-odds of responses “circles” vs. “dipoles” as a function of the number of dipoles for observer O_1. We asked whether the log-odds computed at five within-dipoles distances Δw depended on the distance Δw. To study how log-odds vary with distance Δw we used two models. Model 1 was a single logistic function and Model 2 was a set of five logistic functions, one function per distance Δw. We compared the residual deviances of the two models using a Chi-squared test (Knoblauch & Maloney, 2012). The results for four observers are summarized in Table 1. Model 2 fits the data better for three observers O_1, O_3, O_4 and there is a tendency towards this effect for observer O_2. The results suggest that the number of dipoles at transition points depends on distance Δw for observers O_1, O_3, O_4. This is also demonstrated by Figure 3B, in which the number of dipoles at transition is plotted as a function of distance Δw for four observers.

In Figure 4 results of Experiment 1 are plotted in terms of distance Δb. We tested whether transition distance Δb^*, at which the percepts of “dipoles” and “circles” were equally likely, changed as a function of the within-dipole distance Δw. Because distance Δb was varied jointly with the number of dipoles, we expected that transition distance Δb^* would depend on distance Δw, Indeed, using the same modelling approach as in Figure 3, we found that the

transition distance Δb^* depended on the distance Δw for three observers O_1, O_3, O_4. Results of the statistical tests are summarized in Table 2.

To summarise, in Experiment 1 we found that the transition between the perception of "dipoles" and "circles" depended on spatial distances within and between the dipoles. At small distances Δw, transition ratios $R^* = \Delta b/\Delta w$ were greater than unity, in violation of the principle of proximity. In the next experiment we separate the effect of the number of dipoles from the effect of dot proximity.

Experiment 2: Object identity does not depend on the number of dipoles

Experiment 2 consisted of two parts. In Experiment 2A, we used a display with 18 dipoles and five distances Δw (0.15, 0.25, 0.38, 0.64 and 1.28 deg). Distance Δb was manipulated by varying the dipole eccentricity, i.e. by varying the distance between the dipoles and the screen center. The results of Experiment 2A are plotted in Figure 5. In Figure 5A, the transition ratios R^* are plotted as a function of distance Δw for two observers (one naïve and one of the authors). Just as in Experiment 1, the transition ratios were a decreasing function of distance Δw, indicating that it was not the number of dipoles that determined transition ratios. In Figure 5B, the transition distances Δb^* are plotted as a function of within-dipole distance Δw. Using the same modelling approach as in Experiment 1, we found a significant effect of distance Δw. Results of statistical tests are summarized in Table 3.

In Experiment 2B, we used displays with four numbers of dipoles (4, 7, 10, and 18) which yielded four distances Δb: 4.71, 2.69, 1.88 and 1.25 deg. To find the points of transition between "dipoles" and "circles," we varied the within-dipole distance Δw in an adaptive procedure. Because of the procedure, each observer was presented with different distances Δw. The results for four naïve observers are shown in Figure 6. Observers were not able to achieve a transition point at the distance Δb of 4.71. For the remaining distances Δb, the transition ratios were a decreasing function of distance Δw, similar to Experiment 1. This result indicates that the transition ratios depend on the distances within and between the dipoles.

Interim discussion

In Experiments 1 and 2 we studied the perception of object identity as a function of spatial proximity. We computed the transition ratios as the ratios of distances between and within the dipoles at which two alternative interpretations of the display were equally likely. We found that the transition ratios were larger than unity, which indicates that grouping violated the Gestalt principle of proximity.

Since in Experiment 1 the effect of proximity was confounded with the effect of the number of the dipoles, in Experiment 2 we tested the effect of proximity independently of the number of the dipoles. We showed that the transition ratios were controlled by the proximity between and within dipoles and not by the number of dipoles.

In Experiments 1 and 2 we focused on the effect of proximity, although perception of our displays could have depended on other grouping factors. One of these factors is common

motion, called “common fate” (Wertheimer, 1923), which implies that the dots that move in the same directions and with the same speeds are likely to be perceived as parts of the same object. Our displays could be seen two ways, as “rotating dipoles” or “pulsating circles.” Of the two organizations, the latter was supported by common motion (whereas the former was not) making the perception of “pulsating circles” more likely than the perception of “rotating dipoles.” However, the trajectories and speeds of dots within each organization did not change as we manipulated the proximity within and between the dipoles. In other words, we manipulated the proximity of dots but not their common motion, and we observed significant changes in perception. This suggests that it was dot proximity rather than their common motion that determined perception in Experiments 1 and 2.

Similarly, it is dot proximity and not common motion that controls perception of the Ternus display (1926) described in Figure 1A. The Ternus display can be perceived either as element motion or group motion. Element motion is seen when one dot appears to hop left and right while the second dot appears to be static. Group motion is seen when the dots appear to move left and right together, in agreement with common motion because both dots appear to move in the same direction with the same speed. In several studies with the Ternus display the effect of common motion was kept the same and the spatiotemporal proximity between the dots was varied. Decreasing the temporal distance between frames made perception of group motion less likely whereas decreasing the spatial distance between the dots made perception of group motion more likely (Petersik & Pantle, 1979; He & Ooi, 1999). These findings are consistent with the notion that perception of the Ternus display was also determined by dot proximity rather than common motion.

An earlier study suggested that in the display with rotating dipoles, the perception of “dipoles” vs. “circles” follows the Gestalt principle of proximity, but the effect of proximity can be overwritten by the feature similarity (Anstis & Kim, 2011). Our experiments showed that even though perception of these displays depends on the inter-dot distances, perception did not always follow the principle of proximity. This results is consistent with the findings in another type of discrete visual display called “motion lattice,” described in Figure 1B (Gepshtein & Kubovy, 2007). Spatiotemporal grouping in motion lattices was also shown to violate the proximity principle at high speed of apparent motion. Gepshtein & Kubovy (2007) observed that a function that described spatiotemporal grouping in motion lattices had a shape similar to the shape of the spatiotemporal contrast sensitivity function (Kelly, 1979), helping to resolve several inconsistencies in the literature on apparent motion (Koffka & Korte, 1915; Koffka, 1935; Burt & Sperling, 1981). Gepshtein & Kubovy (2007) proposed that grouping of suprathreshold stimuli and detection of threshold stimuli followed similar principles. In the next section we ask whether this notion applies to perception of object identity.

Predictions from contrast sensitivity

The contrast sensitivity function describes how the contrast of a just detectable drifting luminance grating varies with spatial and temporal frequencies of the grating (Figure 7A; Kelly, 1979). The different sensitivity for different stimulus conditions is commonly interpreted in terms of the uneven allocation of the neural mechanisms (“motion detectors”)

tuned to these conditions (De Valois, Albrecht, & Thorell, 1982; Silverman, Grosof, De Valois, & Elfar, 1989; Priebe, Lisberger, & Movshon, 2006). Standard models of motion detectors include several subunits. The subunits represent cells or circuits which are tuned to stimulus locations separated by spatial distance d_s, while the outputs of subunits are combined with a time lag d_t. The magnitudes of d_s and d_t determine the detector's selectivity for speed (van Santen & Sperling, 1985; Watson & Ahumada, 1985; Heess & Bair, 2010). The subunits are tuned to the same spatial frequency of the stimulus, with a $\pi/2$ phase shift, which makes the detectors most sensitive to the apparent motion with the displacement of one quarter of stimulus period (van Santen & Sperling, 1985; Heess & Bair, 2010). That is, a continuously moving luminance grating with the spatial and temporal periods S and T will evoke the same response of the detector as a grating displaced discretely for the distance of $S/4$ over the temporal interval of $T/4$ (van Santen & Sperling, 1985; Heess & Bair, 2010).

In agreement with these studies, Nakayama (1985) showed that the sensitivity to continuously drifting luminance gratings with spatial and temporal periods S and T was similar to the sensitivity to apparent motion of discrete elements other than gratings displaced over spatial distance $S/4$ and temporal interval $T/4$. Accordingly, the property of the visual system manifested in the contrast sensitivity function can also be represented in the coordinates of spatial and temporal distances.

Following these arguments, in Figure 7 we mapped the contrast sensitivity function from the coordinates of spatiotemporal frequencies (Figure 7A) to the coordinates of spatiotemporal distances (Figure 7B) such that spatial frequency F_s corresponded to spatial distance of $(4F_s)^{-1}$ and temporal frequency F_t corresponded to temporal distance of $(4F_t)^{-1}$ (Nakayama, 1985; Gepshtein & Kubovy, 2007).

In the contrast sensitivity function in Figure 7A, the sensitivity to drifting luminance gratings with spatial and temporal frequencies is represented in the coordinates of gratings parameters F_s and F_t. in Figure 7B, we represent the same results in the coordinates of spatiotemporal distances. That is, the sensitivity to gratings with spatial frequency F_s and temporal frequency F_t is mapped to the coordinates of $D_s = (4F_s)^{-1}$ and $D_t = (4F_t)^{-1}$. The function in Figure 7B can be used to predict the relative strengths of alternative spatiotemporal groupings over different spatial and temporal distances D_s and D_t. For example, Gepshtein & Kubovy (2007) studied displays in which grouping of dots over different spatiotemporal distances evoked perception of motion in different directions. In some conditions, *increasing* spatiotemporal distances made perception of motion more likely. This result was consistent with results of studies concerned with the threshold of visibility of drifting luminance gratings. Gepshtein & Kubovy (2007) represented the contrast sensitivity in the coordinates D_s and D_t. Each pair of stimulus parameters D_s and D_t was deemed to correspond to a motion detector most sensitive to these parameters. The conditions of equal sensitivity corresponded to conditions at which two apparent motions were equally likely. Using this approach, we asked whether the function in Figure 7B can explain the paradoxical grouping observed in Experiments 1 and 2. That is, we asked whether the transition ratios in our displays could be predicted from Figure 7B, as the following.

In Figure 8 we plot a "slice" of the function portrayed in Figure 7B, where it is marked by a horizontal line at Δt = 170 ms. In Figure 8A, we identify two spatial distances that correspond to the same contrast sensitivity, indicated by the upper gray line for distances Δw_1 and Δb_1 and by the lower gray line for distances Δw_2 and Δb_2. In Figure 8B, we plot the predicted transition ratios $R^*_{pred} = \Delta b/\Delta w$ against distance Δw. The function that fits the predictions in Figure 8B has the form $k/\Delta w$, where k is a free parameter. The empirical transition ratios found in Experiments 1 and 2 (Figure 2 and Figure 4) followed the same qualitative pattern.

Experiment 3: Validation of mapping between frequencies and distances

In the previous experiment we found that the paradoxical spatiotemporal grouping observed in Experiments 1 and 2 could potentially be predicted from the pattern of spatiotemporal contrast sensitivity in Figure 7B. This pattern was obtained by mapping the conditions of equal sensitivity from the coordinates of spatiotemporal frequencies to the coordinates of spatiotemporal distances. The transformation was performed using a "mapping rule" derived from the standard model of motion detector. The rule was used previously to predict perception of two-frame apparent motion displays (Nakayama & Silverman, 1985; Nakayama, 1985). However, Watson (1990) proposed that a different mapping rule could apply in multifame displays. Here we test whether the same rule can be used to predict perception of our multifame displays.

Methods

Individual grouping preferences were measured using displays with rotating dipoles. The temporal distance between the successive frames was 170 ms. Within-dipole distances Δw were 0.15, 0.25, 0.38, 0.64 and 1.28 deg. The radius of the invisible circle on which we positioned the dipoles was 3 deg. The between-dipole distance Δb was manipulated by changing the number of dipoles.

Individual contrast sensitivities were measured using horizontally drifting sinusoidal luminance gratings whose luminance was modulated by a Gaussian function with the spatial constant of 1.5 deg. The gratings appeared on a uniform gray background with the mean luminance of 51.3 cd/m^2. The temporal frequency of gratings was 1.47 Hz and the spatial frequencies were 0.1, 0.3, 0.7, 1.22, 2.45, 4.13, 6.28, 10.47, and 15.00 c/deg. Stimuli were generated using the *mPsy* toolbox (Jurica & Gepshtein, 2014) and presented in blocks of 40 trials. Trials started with a central fixation dot, followed by a drifting luminance grating shown at screen center for 500 msec. The task was to report the perceived direction of drift in the grating using two buttons of a computer mouse. Within a block, the spatial frequency of the grating was constant, while the contrast was controlled by a staircase procedure with a 1-up-3-down rule in the range of [0.004, 1]. Different spatial frequencies of gratings were used in different blocks, the order of blocks randomized across subjects. Within each frequency condition, proportions of correct responses were binned by grating contrast, plotted as a function of contrast, and fitted using a logistic function. Thresholds of direction discrimination were defined as the contrasts at which correct direction discrimination reached 75%. Three naïve observers participated in the experiment.

Results

We obtained individual contrast sensitivity functions by fitting individual estimates of contrast sensitivity (defined as inverse magnitudes of contrast thresholds) using Kelly's equation of contrast sensitivity (Kelly, 1979). In Figure 9A we plot the individual estimates (circles) and the Kelly fit (black line) for one observer. To derive predictions of individual transition ratios from individual contrast sensitivities, we mapped the fitted contrast sensitivity functions from the coordinates of spatial frequencies to the coordinates of spatial distances, using two approaches.

First, we used a theoretical mapping rule based on the standard model of motion detector, as described in section "Predictions from contrast sensitivity." We assumed that the contrast sensitivity function reflects the uneven allocation of neural resources (Gepshtein, Lesmes, & Albright, 2013), i.e., high and low contrast sensitivities arise from, respectively, large and small numbers of motion-sensitive cells tuned to the corresponding spatial and temporal frequencies of stimulation (De Valois et al., 1982; Silverman et al., 1989; Priebe et al., 2006). As mentioned in the section "Predictions from contrast sensitivity", the cells respond to a continuously moving luminance grating just as they respond to the apparent motion of a grating with the same spatial frequency, but displaced by one quarter of the grating period (van Santen & Sperling, 1985; Heess & Bair, 2010). This implies that the cells having equal sensitivity to the continuously moving gratings with spatial frequencies F_{s1} and F_{s2} will also have equal sensitivity to the gratings displaced discretely over spatial distances $D_{s1} = (4F_{s1})^{-1}$ and $D_{s2} = (4F_{s2})^{-1}$. Thus the coordinates of spatiotemporal frequencies can be mapped to the coordinates of spatiotemporal distances according to a rule $D_s = (4F_s)^{-1}$. This "standard mapping rule" is characterized by a mapping constant of 4.

Second, we transformed the coordinates of spatial frequencies to the coordinates of spatial distances using an empirical mapping rule $D_s = (kF_s)^{-1}$, where k was the mapping constant. We found the magnitude of k that minimised the differences between the predicted and measured transition ratios. Thus, the best fitting mapping constant k determines a "fitted mapping rule".

In Figure 9B we plot the predictions derived by the two methods, i.e., using the standard mapping rule (red line) and the fitted mapping rule (green line) for one observer. The figure also contains the measured transition ratios for this observer. Both mapping rules match the measured transition ratios well, summarized in Figure 9. The fitted mapping constant of 4.54 (which yields the best match to the measured transition ratios for this observer) is close to the "standard mapping constant" of 4.0.

In Figure 10, we illustrate how the fitted mapping constants were selected for three observers. For every observer, we found the mapping constant that yielded the least difference between the predicted and measured transition ratios. The found mapping constants (average 3.6), marked by green vertical lines, are close to the standard mapping constants (4.0), marked by red vertical lines, supporting the conjecture that the standard mapping rule (with constant 4.0) can be used for predicting perception of our displays.

To summarize, in Experiment 3 we found a good correspondence between the individual transition ratios measured in our display and the predictions derived from the individual contrast sensitivity functions. In agreement with previous studies, the mapping constant based on the standard model of motion detector can serve as a useful rule of thumb for mapping between the parameters of discrete and continuous stimuli.

Experiment 4: Object identity as a function of spatiotemporal distances

In Experiments 1 and 2 we studied perception of object identity as a function of spatial proximity between the dots. Perception of object identity violated the proximity principle but it corresponded to predictions from the contrast sensitivity function. In Experiment 4 we studied how object identity is affected by the *spatiotemporal* proximity.

Methods

We used six temporal distances Δt (17, 34, 68, 102, 170 and 340 ms) and two within-dipole distances Δw (0.38 and 0.64 deg), presenting 100 trials per condition. The radius of the invisible circle was 3 deg and between-dipole distance Δb was manipulated by changing the number of dipoles. Four observers participated in the experiment: three naïve and one of the authors (AZ).

Results

Figure 11 is a plot of the transition ratios R^* measured in Experiment 4. The transition ratios for $\Delta w = 0.38$ deg were larger than those for $\Delta w = 0.64$ deg. Again, perception of the display violated the principle of spatiotemporal proximity: decreasing the distance within dipoles increased the transition ratios.

We asked whether this paradoxical grouping can be explained by the spatiotemporal contrast sensitivity function summarized by Kelly (1979). The predicted transition ratios $R^*_{pred} = \Delta b/\Delta w$ are illustrated in Figure 12A for $\Delta w = 0.38$ deg at temporal distances Δt_1 and Δt_2. We found sensitivity at point $(\Delta w, \Delta t_1)$ and then obtained Δb_1 for which the sensitivity was the same as at $(\Delta w, \Delta t_1)$ (Figure 12A). Figure 12B is a plot of the transition ratios R^*_{pred} as a function of temporal distance. The transition ratios increase until they reach a maximum at the temporal distance of 50–70 ms, and they decrease for larger temporal distances.

Empirical transition ratios agreed with the predictions. However, the empirical transition ratios found in Experiment 4 did not match the predicted ratios as well as in Experiments 1 and 2. In the latter, the transition ratios were derived from a single section of the sensitivity function, while in Experiment 4 the transition ratios were derived from several sections of the sensitivity function and they reflected the shape of this function. The discrepancy may arise from individual variability in contrast sensitivity. Contrast sensitivity functions of individual observers may have parameter values different from the values for the averaged contrast sensitivity function obtained by Kelly (1979). In Figure 13, we illustrate how different shapes of individual contrast sensitivity functions could produce transition ratios similar to our results. According to Kelly (1979), the contrast sensitivity function has the following form:

$$C = k v \alpha^2 \exp(-2\alpha/\alpha_{max}),$$

where v is stimulus speed, α is the spatial frequency, and k and α_{max} are speed-dependent coefficients:

$$k = 6.1 + 7.3|\log(v/3)|^3,$$
$$\alpha_{max} = 45.9/(v+2).$$

Parameter α_{max} determines the location of the maximal sensitivity and k determines the steepness of sensitivity function.

We asked what range of parameters of the Kelly function could account for the results shown in Figure 11. We fitted the Kelly function to the observed transition ratios by varying k and α_{max}. Figure 13 portrays three modified contrast sensitivity functions that matched the results of Experiment 4. We plot contrast sensitivity functions in the top row and predictions from these functions in the bottom row. The coefficients are $\alpha_{max} = 49.9/(v + 2)$ and $k = 6.1 + 7.3|\log(v/3)|^3$ in panels A and B; $\alpha_{max} = 70/(v + 2)$ and $k = 1 + |\log(v/3)|^3$ in panels C and D; $\alpha_{max} = 21/(v + 2)$ and $k = 3.44 + |\log(v/3)|^3$ in panels E and F.

To summarize, in Experiment 4 we studied perception of object identity as a function of spatiotemporal proximity between the dots. The transition ratios agreed qualitatively with the predictions from the Kelly function: the transition ratios were larger when distance Δw was smaller, but transition ratios varied between individual observers and differed from the predictions quantitatively. The disagreement between the transition ratios and predictions from the contrast sensitivity function could be explained by individual variability of individual contrast sensitivities. In Figure 13, we plot three possible variants of the Kelly function that could produce a pattern of transition ratios consistent with our results. Future studies should test this hypothesis by measuring the spatiotemporal contrast sensitivity functions individually and testing whether predictions derived from the individual contrast sensitivity functions would agree with perception of object identity.

Discussion

We studied perception of object identity in dynamic visual displays. We used a bistable display in which alternative groupings of display elements corresponded to different object identities. We found that in these displays the effect of spatiotemporal proximity between the dots was inconsistent with the Gestalt principle of proximity. In some conditions, increasing the spatiotemporal distance between the dots made their grouping more likely, while the proximity principle states that grouping over shorter distances is always more likely.

Instead of the proximity principle, we found that perceived object identity was predicted by a threshold characteristic of vision: the contrast sensitivity function. This function is measured using luminance gratings (Kelly, 1979; Campbell & Gubisch, 1966; Campbell & Robson, 1968) and it is commonly viewed as a description of the mechanisms responsible for encoding and perception of motion in the mammalian visual pathways, from retina to

motion-sensitive areas of the visual cortex (De Valois et al., 1982; Desimone, Albright, Gross, & Bruce, 1984; Rodman & Albright, 1989; Priebe et al., 2006). We rendered the contrast sensitivity function in terms of spatial and temporal distances rather than spatiotemporal frequencies (Nakayama, 1985; Gepshtein & Kubovy, 2007; Heess & Bair, 2010) using a mapping rule derived from a standard model of motion detection. We used the conditions of equal contrast sensitivity plotted in the coordinates of spatial and temporal distances to predict the conditions of perceptual equilibrium for object identity.

Our findings generalize results of a previous study, using different apparent motion displays, where perceptual organization also contradicted the principle of proximity. Gepshtein & Kubovy (2007) used motion lattices in which the dots were arranged in a periodic pattern and appeared to move all in the same direction along a linear trajectory, forming no distinct shapes. In some conditions, the dots separated by longer spatial distance between the frames were more likely to be grouped and thus to evoke the perception of motion. Here we report that the failure of the proximity principle generalizes to displays in which the elements follow curvilinear trajectories and group into distinct shapes.

It may be surprising that perception of shape in suprathreshold discontinuous stimuli can be predicted from a threshold characteristic of vision obtained using continuous stimuli. Perception of object identity is generally expected to depend on mid-level visual processes, distinct from the lower-level processes responsible for encoding of luminance contrast (Wertheimer, 1923; Marr, 1976; Nakayama, He, & Shimojo, 1995). The low-level processes are thought to determine what information is available for mid-level analysis. For example, visual systems encode only a limited range of spatial and temporal frequencies of luminance modulation in the optical stimuli: a notion described by Watson & Ahumada (1983) as a “window of visibility.” Watson & Ahumada (1983) used this notion to explain the relationship between the perception of motion in continuous and discontinuous stimuli. The contrast sensitivity function could be regarded as a graded window of visibility that reflects the degree to which different components of the stimulus are attenuated. Accordingly, the contrast sensitivity function can be used to characterize the relationship between continuous and discontinuous stimuli because the function captures the extent to which visual systems attenuate those high-frequency components that distinguish continuous stimuli from fragmented ones.

The relationship between perception of threshold and suprathreshold stimuli has also been studied using the technique of contrast matching. Early studies found that apparent contrast did not depend on spatial and temporal frequencies of luminance modulation: a phenomenon called “contrast constancy” (Georgeson & Sullivan, 1975; Georgeson, 1987; Webster, Georgeson, & Webster, 2002). Recent studies contested this conclusion, however, and found that apparent contrast did vary across spatiotemporal frequencies, reflecting the perception near threshold (Bex & Langley, 2007; Smith, 2015). Our finding that perception of suprathreshold stimuli varies across spatiotemporal stimuli agrees with the observations of failure of contrast constancy.

The correspondences between perception of threshold and suprathreshold stimuli, as well as between perception of continuous and apparent motion, have been anticipated in a

theoretical study of constraints of visual measurement. Gepshtein, Tyukin & Kubovy (2007) traced the expected uncertainty of motion measurement across the full range of spatial and temporal sizes of visual receptive fields and found that the distribution of expected uncertainty had a shape similar to the shape of the distribution of contrast sensitivity captured by the Kelly function (1979), plotted in our Figure 7. The authors proposed to view this function as a manifestation of a process that allocates neural resources–according to the expected uncertainty of measurement. Such efficient allocation would reduce the aggregate error of visual measurement. Jurica et al. (2013) demonstrated how the efficient allocation could arise by adaptive tuning of motion-sensitive mechanisms. According to their model, the variable motion sensitivity corresponds to a variable density of motion-sensitive mechanisms allocated to different stimulus conditions. The more of these mechanisms are tuned to certain stimuli, the higher the sensitivity to these stimuli. On this view, several characteristics of visual performance are expected to have similar shapes, including the contrast sensitivity function (which describes perception at the threshold of visibility) and the characteristics obtained in the present study (which describe perception in suprathreshold displays).

Although grouping preferences were in general agreement with the contrast sensitivity function, they were subject to considerable between-observer variability. This variability may correspond to individual differences in contrast sensitivity, shaped by the adaptation to the varying statistics of visual stimulation (De Valois, 1977; Wainwright, 1999; Solomon, Peirce, Dhruv, & Lennie, 2004; Kohn, 2007; Gepshtein et al., 2013). Future research should reveal whether individual variation in contrast sensitivity matches the individual characteristics of perceptual organization.

Supplementary Material

Refer to Web version on PubMed Central for supplementary material.

Acknowledgments

We thank V. Ekroll and E. Steur for helpful comments on an earlier version of the manuscript. This work was supported by Odysseus grant from the Flemish Society for Research (FWO) (to C.v.L.); by National Institutes of Health Grant EY018613 and National Science Foundation Grant 1027259 (to S.G.)

References

Anstis S, Kim J. Local versus global perception of ambiguous motion displays. Journal of Vision. 2011; 11(3):13, 1–12.

Bex PJ, Langley K. The perception of suprathreshold contrast and fast adaptive filtering. Journal of Vision. 2007; 7(12):1, 1–23. https://doi.org/10.1167/7.12.1.

Bower T. The development of object permanence: Some studies of existence constancy. Perception & Psychophysics. 1967; (2):416–418.

Burt P, Sperling G. Time, distance and feature trade-offs in visual apparent motion. Psychological Review. 1981; 88(2):171–195. [PubMed: 7291378]

Campbell FW, Gubisch RW. Optical quality of the human eye. The Journal of Physiology. 1966; 186(3):558–578. [PubMed: 5972153]

Campbell FW, Robson JG. Application of Fourier analysis to the visibility of gratings. The Journal of Physiology. 1968; 197(3):551–566. [PubMed: 5666169]

Chun MM. Types and tokens in visual processing: A double dissociation between the attentional blink and repetition blindness. Journal of Experimental Psychology: Human Perception and Performance. 1997; 23(3):738–755. [PubMed: 9180042]

Dawson MR. The how and why of what went where in apparent motion. Psychological Review. 1991; 98(4):569–603. [PubMed: 1961774]

Desimone R, Albright TD, Gross CG, Bruce C. Stimulus-selective properties of inferior temporal neurons in the macaque. The Journal of Neuroscience. 1984; 4(8):2051–2062. [PubMed: 6470767]

De Valois KK. Spatial frequency adaptation can enhance contrast sensitivity. Vision Reseacrh. 1977; 17:1057–1065.

De Valois RL, Albrecht DG, Thorell LG. Spatial frequency selectivity of cells in macaque visual cortex. Vision Research. 1982; 22(5):545–559. [PubMed: 7112954]

Evans DW, Ginsburg AP. Contrast sensitivity predicts age-related differences in highway-sign discriminability. Human Factors: The Journal of the Human Factors and Ergonomics Society. 1985; 27(6):637–642.

Georgeson MA. Temporal properties of spatial contrast vision. Vision Research. 1987; 27(5):765–780. [PubMed: 3660638]

Georgeson MA, Sullivan GD. Contrast constancy: deblurring in human vision by spatial frequency channels. The Journal of Physiology. 1975; 252(3):627–656. [PubMed: 1206570]

Gepshtein S, Kubovy M. The emergence of visual objects in space time. Proceedings of National Academy of Sciences. 2000; 97(14):8186–8191.

Gepshtein S, Kubovy M. The lawful perception of apparent motion. Journal of Vision. 2007; 7(8):9, 1–15. https://doi.org/10.1167/7.8.9.

Gepshtein S, Lesmes LA, Albright TD. Sensory adaptation as optimal resource allocation. Proceedings of National Academy of Sciences. 2013; 110(11):4368–4373.

Gepshtein S, Tyukin I, Kubovy M. The economics of motion perception and invariants of visual sensitivity. Journal of Vision. 2007; 7(8):8, 1–18. https://doi.org/10.1167/7.8.8.

Ginsburg AP, Evans DW, Cannon MWJ, Owsley C, Mulvanny P. Large-sample norms for contrast sensititivity. American Journal of Optometry and Physiological Optics. 1984; 61(2):80–84. [PubMed: 6703012]

Heess N, Bair W. Direction opponency, not quadrature, is key to the 1/4 cycle preference for apparent motion in the motion energy model. Journal of Neuroscience. 2010; 30(34):11300–11304. [PubMed: 20739550]

He ZJ, Ooi TL. Perceptual organization of apparent motion in the Ternus display. Perception. 1999; 28:877–892. [PubMed: 10664779]

Hochberg, J. Handbook of perception. Academic Press; New-York & London: 1974. Organization and the Gestalt tradition; p. 179-210.

Hochberg, J. Perception of motion pictures. In: Gregory, RL., Zangwill, OL., editors. The Oxford companion to the mind. Oxford: Oxford University Press; 1987. p. 604-608.

Jones EE, Bruner JS. Expectancy in apparent visual movement. British Journal of Psychology. 1954; 45:157–165. [PubMed: 13190168]

Jurica, P., Gepshtein, S. Modular psychophysics in Python. GitHub Repository. 2014. Retrieved from https://github.com/wisions/mPsy

Jurica P, Gepshtein S, Tyukin I, van Leeuwen C. Sensory optimization by stochastic tuning. Psychological Review. 2013; 120(4):798–816. [PubMed: 24219849]

Kahneman D, Treisman A, Gibbs BJ. The reviewing of object files: Object-specific integration of information. Cognitive Psychology. 1992; 24(2):175–219. [PubMed: 1582172]

Kellman PJ, Spelke ES. Perception of partly occluded objects in infancy. Cognitive Psychology. 1983; (15):483–524. [PubMed: 6641127]

Kelly DH. Motion and Vision. II. Stabilized spatio-temporal threshold surface. Journal of the Optical Society of America. 1979; 69(10):1340–1349. [PubMed: 521853]

Knoblauch, K., Maloney, LT. Modeling psychophysical data in R. Springer; New York: 2012.

Koffka, K. Principles of Gestalt psychology. 5. Routledge & Kegan Paul; London: 1935.

Koffka K, Korte A. Beitrage zur Psychologie der Gestalt- und Bewegungserlebnisse. Zeitschrift Fur Psychologie. 1915; 72:194–297.

Kohn A. Visual Adaptation: Physiology, Mechanisms, and Functional Benefits. Journal of Neurophysiology. 2007; 97(5):3155–3164. [PubMed: 17344377]

Kontsevich LL, Tyler CW. Bayesian adaptive estimation of psychometric slope and threshold. Vision Research. 1999; 39:2729–2737. [PubMed: 10492833]

Kramer P, Yantis S. Perceptual grouping in space and time: Evidence from the Ternus display. Perception & Psychophysics. 1997; 59(1):87–99. [PubMed: 9038411]

Kubovy M, Wagemans J. Grouping by proximity and multistability in dot lattices: A quantitative gestalt theory. Psychological Science. 1995; 6(4):225–234.

Marr D. Early processing of visual information. Philosophical Transactions of the Royal Society B. 1976; 275:483–524.

Moore CM, Stephens T, Hein E. Features, as well as space and time, guide object persistence. Psychonomic Bulletin & Review. 2010; 17:731–736. [PubMed: 21037174]

Nakayama K. Biological image processing. Vision Research. 1985a; 25(5):625–660. [PubMed: 3895725]

Nakayama K. Biological image processing. Vision Research. 1985b; 25(5):625–660. [PubMed: 3895725]

Nakayama, K., He, ZJ., Shimojo, S. Osherson Vision. Visual surface representation: A critical link between Lower-level and Higher-level vision. In: Kosslyn, SM., DN, editors. An Invitation to cognitive Science. 1995. p. 1-70.

Oyama T. Perceptual grouping as a function of proximity. Perceptual and Motor Skills. 1961; 13:305–306.

Peirce JW. PsychoPy - Psychophysics software in Python. Journal of Neuroscience Methods. 2007; 162(1–2):8–13. [PubMed: 17254636]

Petersik JT, Pantle A. Factors controlling the competing sensations produced by a bistable stroboscopic motion display. Vision Research. 1979; 19:143–154. [PubMed: 425333]

Peterzell DH, Teller DY. Individual differences in contrast sensitivity functions: the lowest spatial frequency channels. Vision Reseacrh. 1996; 36(19):3077–3085.

Peterzell DH, Werner JS, Kaplan VS. Individual differences in contrast sensitivity functions: longitudinal study of 4-, 6- and 8-month-old human infants. Vision Reseacrh. 1995; 35:961–979.

Pomerantz JR, Portillo MC. Grouping and emergent features in vision: Toward a theory of basic Gestalts. Journal of Experimental Psychology: Human Perception and Performance. 2011; 37(5): 1331–1349. [PubMed: 21728463]

Priebe NJ, Lisberger SG, Movshon JA. Tuning for spatiotemporal frequency and speed in directionally selective neurons of macaque striate cortex. Journal of Neuroscience. 2006; 26(11):2941–2950. [PubMed: 16540571]

Rodman HR, Albright TD. Single-unit analysis of pattern-motion selective properties in the middle temporal visual area (MT). Experimental Brain Research. 1989; 75:53–64. [PubMed: 2707356]

Silverman MS, Grosof DH, De Valois RL, Elfar SD. Spatial-frequency organization in primate striate cortex. Proceedings of the National Academy of Sciences. 1989; 86(2):711–715.

Smith WS. Contrast constancy revisited: The perceived contrast of sinusoidal gratings above threshold. The Quarterly Journal of Experimental Psychology. 2015; 68(2):363–380. [PubMed: 25026464]

Solomon SG, Peirce JW, Dhruv NT, Lennie P. Profound contrast adaptation early in the visual pathway. Neuron. 2004; 42(1):155–162. [PubMed: 15066272]

Ternus, J. A Source Book of Gestalt Psychology. Routledge & Kegan Paul; London: 1926. The problem of phenomenal identity. English translation; p. 149-160.

Tukey, JW. Exploratory data analysis. Reading, Massachusetts: Addison-Wesley Publishing Company; 1977.

van Santen J, Sperling G. Elaborated Reichardt detectors. Journal of the Optical Society of America A. 1985; 2(2):300–321.

Wainwright MJ. Visual adaptation as optimal information transmission. Vision Research. 1999; 39(23):3960–3974. [PubMed: 10748928]

Watson, AB., Ahumada, AJJ. NASA Technical Memorandum 84352. 1983. A look at motion in the frequency domain.

Watson AB, Ahumada AJJ. Model of human visual-motion sensing. Journal of the Optical Society of America. 1985; 2(2):322–341. [PubMed: 3973764]

Webster MA, Georgeson MA, Webster SM. Neural adjustments to image blur. Nature Neuroscience. 2002; 5(9):839–840. [PubMed: 12195427]

Wertheimer, M. A Source Book of Gestalt Psychology. Routledge & Kegan Paul; London: 1923. Laws of organization in perceptual forms; p. 71-88.

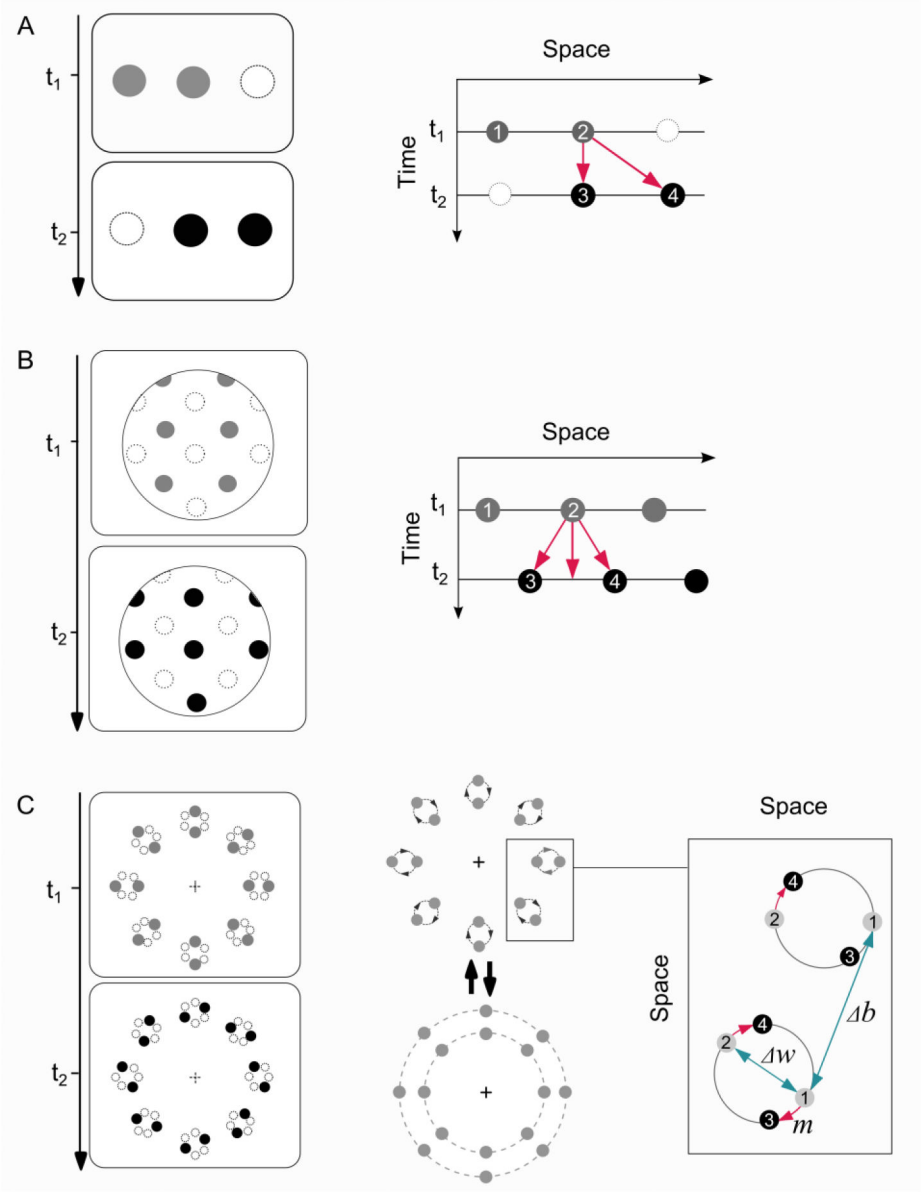

Figure 1.

Motion displays. Dots 1 and 2 appear in the first frame (grey); dots 3 and 4 appear in the second frame (black). Red arrows indicate possible groupings across frames. (A) The Ternus display. Left: two subsequent frames of the display. Right: event diagram. Grouping {2,3} represents "element motion" and grouping {2,4} represents "object motion" where dots 1 and 2 move together, as a single entity. (B) Motion lattice. Left: two subsequent frames of motion lattice. Right: event diagram. Groupings {2,4} and {2,3} corresponds to element motion. Grouping of rows of dots (represented by the vertical arrow) corresponds to downward group motion. (C) Display used in the present study. Blue arrows indicate possible dot groupings within frames. Left: two subsequent frames of the display. Middle: two alternative percepts of the display: multiple rotating dipoles vs. two pulsating circles (illustrated in Movies 1 and 2). Right: diagram of two dipoles. Distance Δw separates dots

within the dipole, distance Δb separates dots in adjacent dipoles, distance m separates dots between successive frames. Grouping over distance Δw corresponds to perception of dipoles and grouping over distance Δb corresponds to perception of circles.

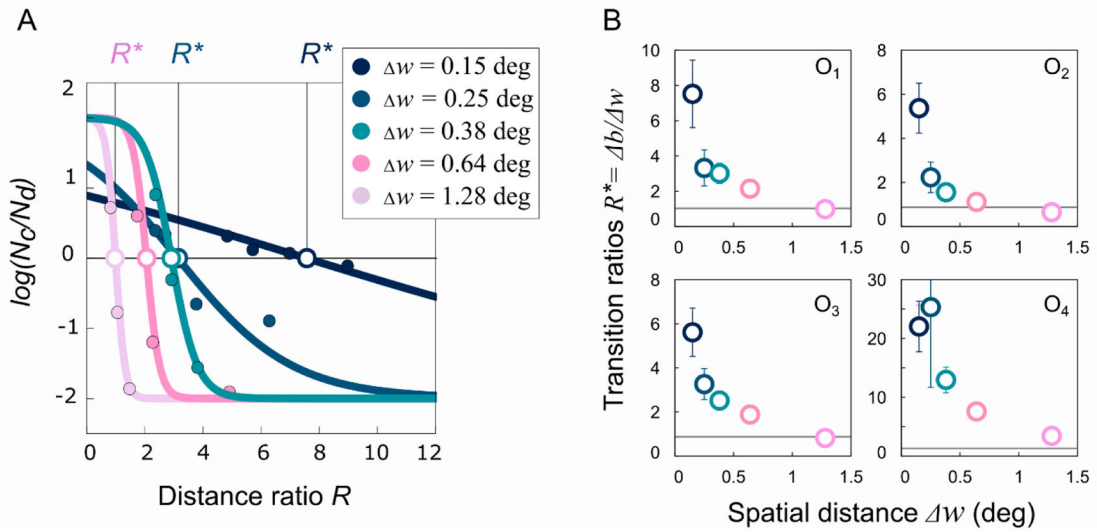

Figure 2.

Results of Experiment 1. (A) Method for finding the transition ratios. Log-odds of the responses "circle" and "dipoles" are plotted as a function of distance ratio $R=\Delta b/\Delta w$ for observer O_1 at five within-dipole distances Δw. Transition ratio R^* is the magnitude of R at zero log-odds of percepts "circles" and "dipoles". (B) Transition ratios are plotted as a function of distance Δw. The grey line marks the transition ratios of unity. If grouping followed the proximity principle, the transition ratios would fall on this line. Error bars represent ±1 SE; they are visible only when larger than the data symbols.

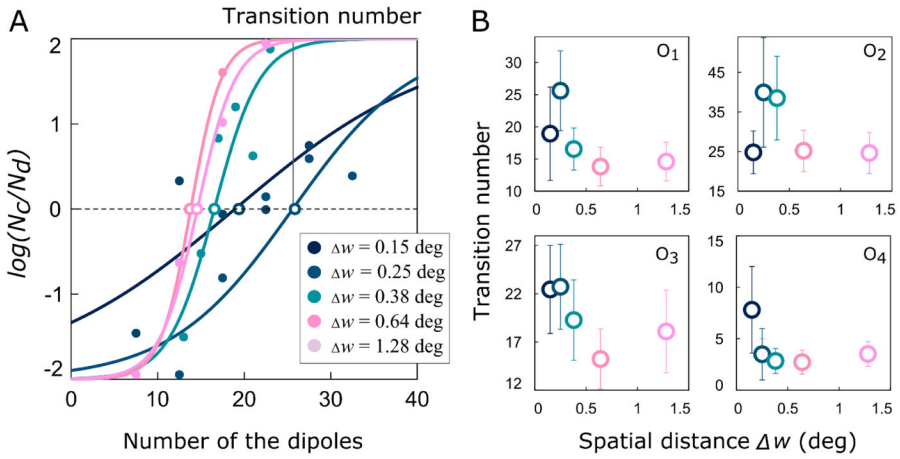

Figure 3.

Results of Experiment 1 plotted in terms of the number of dipoles. (A) Log-odds of the responses “circle” and “dipoles” are plotted as a function of the number of dipoles at five within-dipole distances Δw for observer O_1. Log-odds are fitted best with a model with five thresholds, rather than a single threshold. (B) Number of the dipoles at the transition points is plotted as a function of within-dipole distance Δw. Error bars represent ±1 SE.

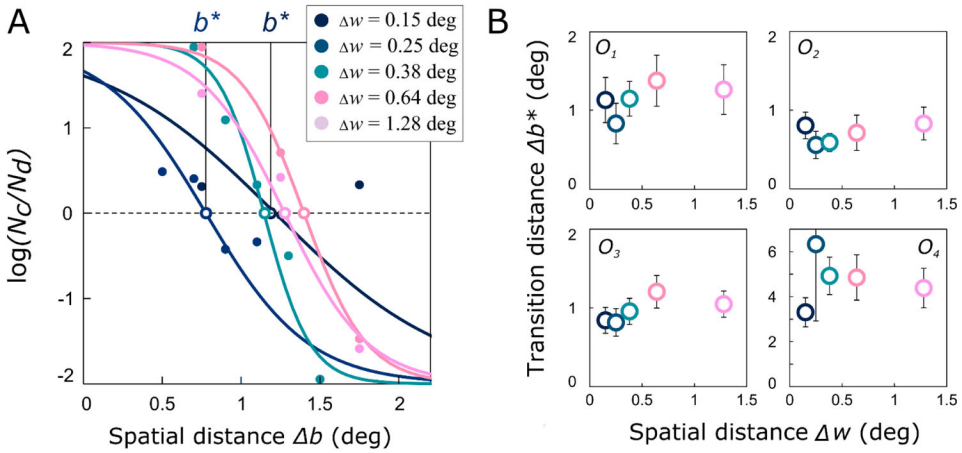

Figure 4.

Results of Experiment 1 plotted in terms of distance *Δb*. (A) Log-odds of the responses "circle" and "dipoles" are plotted as a function of distance *Δb* for observer O_1 at five within-dipole distances *Δw*. Log-odds are fitted best with a model with five thresholds, rather than a single threshold. Transition distance *Δb** is the magnitude of *Δb* at zero log-odds of percepts "circles" and "dipoles". (B) Transition distances *Δb** are plotted as a function of distance *Δw*. Error bars represent ±1 SE.

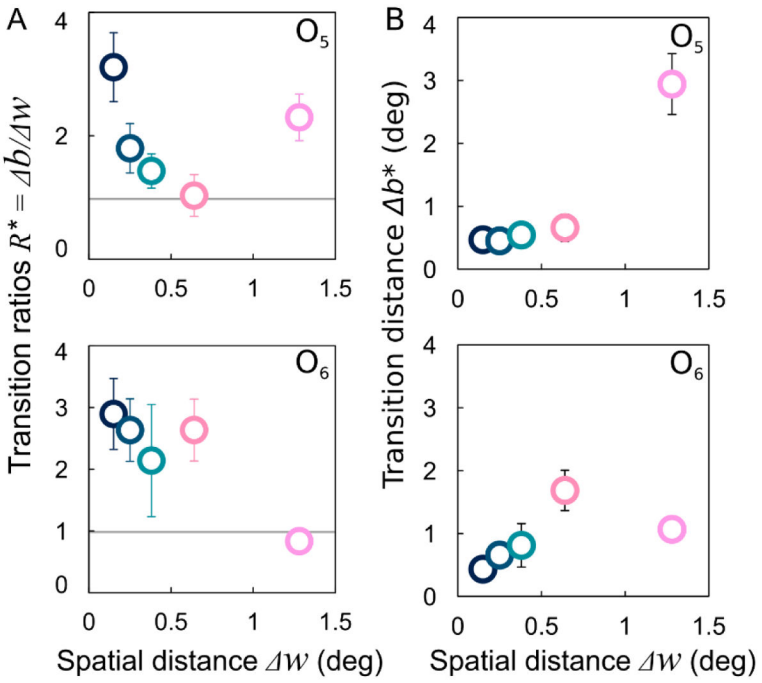

Figure 5.

Results of Experiment 2A. The between-dipole distance *Δb* was varied by changing dipole eccentricity. (A) Transition ratios are plotted as a function of within-dipole distance *Δw*. The grey horizontal line marks the transition ratio *R** of unity. If grouping followed the proximity principle, then *R** would fall on this line. Error bars are ±1 SE, visible only when larger than data symbols. (B) The transition distances *Δb** are plotted as a function of the within-dipole distance *Δw*.

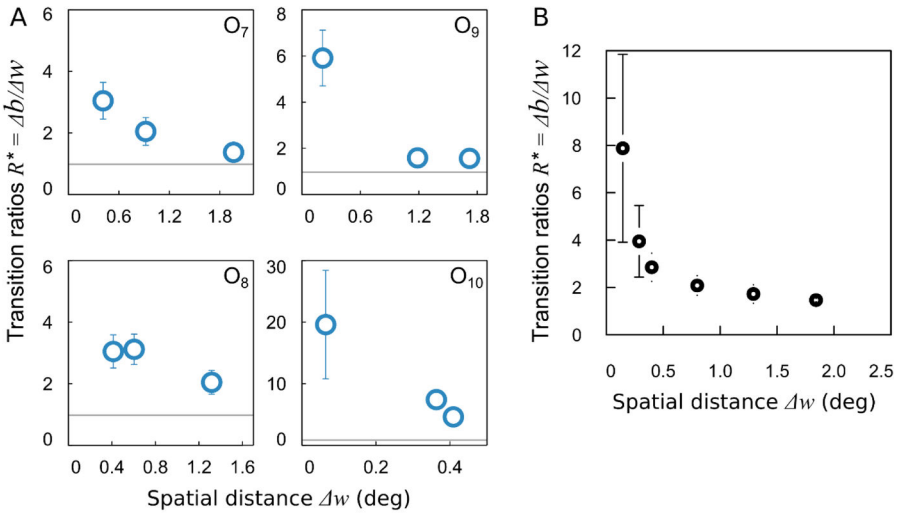

Figure 6.

Results of Experiment 2B, in which the within-dipole distance Δw was varied. (A) Transition ratios R^* are plotted as a function of distance Δw for observers O7–O10. The grey lines mark the transition ratios of unity. Error bars represent ±1 SE visible only when larger than the data symbols. (B) Transition ratios R^* averaged across observers O7–O10 using data binning.

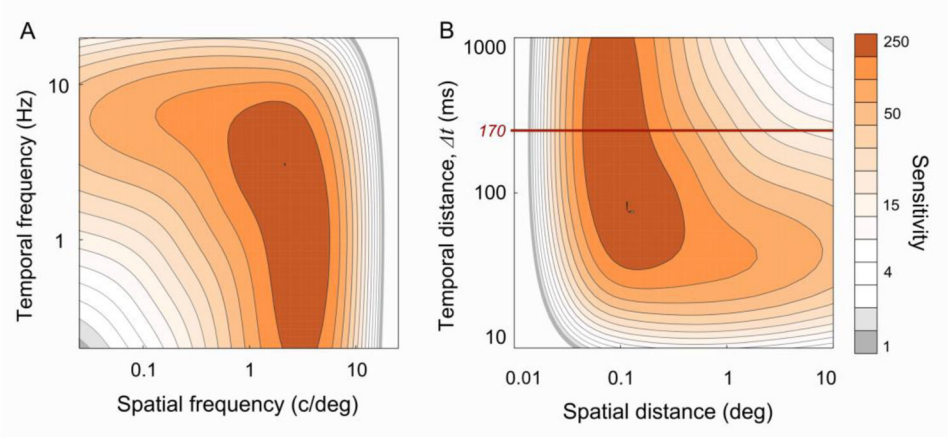

Figure 7.

Human spatiotemporal contrast sensitivity rendered in coordinates of spatiotemporal frequency (A) and in coordinates of spatial and temporal distances (B). The contours connect the conditions of the same sensitivity. The horizontal line is a section through the contrast sensitivity function at $\Delta t = 170$ ms.

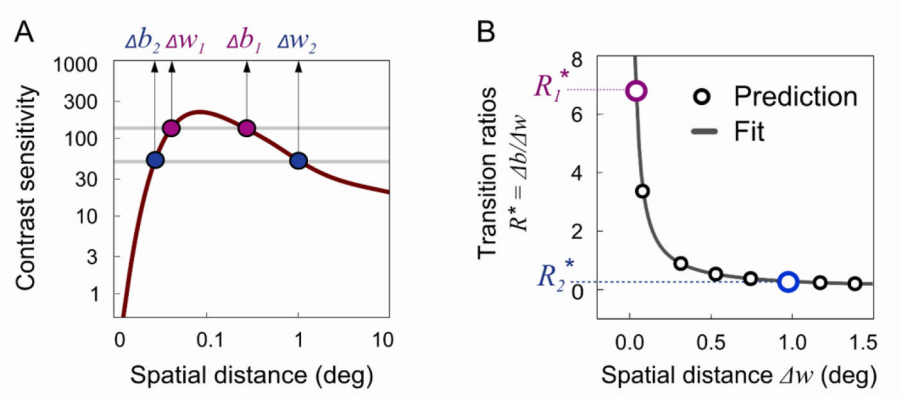

Figure 8.

Predictions for Experiments 1 and 2. (A) Contrast sensitivity at $\Delta t = 170$ ms is plotted as a function of spatial distance. Dots of the same color indicate distances Δb and Δw corresponding to the same sensitivity. (B) Transition ratios $R^* = \Delta b/\Delta w$ are plotted against distance Δw, interpolated with function $k/\Delta w$, where k is a free parameter. R_1^* and R_2^* are ratios of distances Δb and Δw indicated in panel (A).

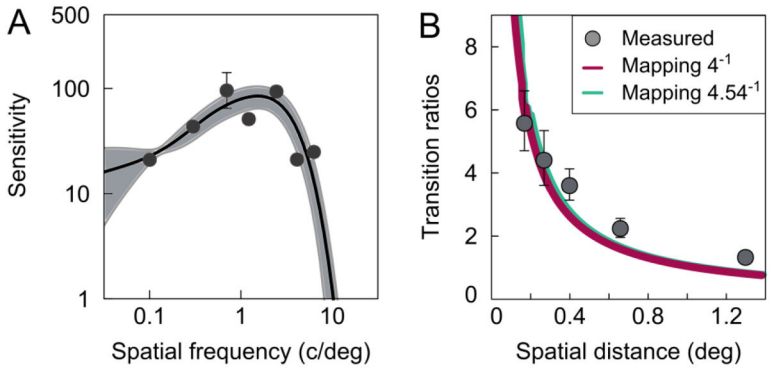

Figure 9.

Comparison of individual grouping preferences and individual contrast sensitivities. (A) Spatial contrast sensitivity function (CSF) for Observer 7. The circles and the curve represent estimates of contrast sensitivity and the best fit by the Kelly equation. The grey region marks one standard error of the fit. (B) The circles stand for measured transition ratios plotted as a function of spatial distance between dots within dipoles for the same observer as in panel A. The red and green lines are transition ratios predicted from the CSF in panel A using two rules: the “standard mapping rule” expected from the standard model of motion detector (mapping constant 4) and the “fitted mapping rule” rule that best fits the measured transition ratios (mapping constant 4.54 for this observer).

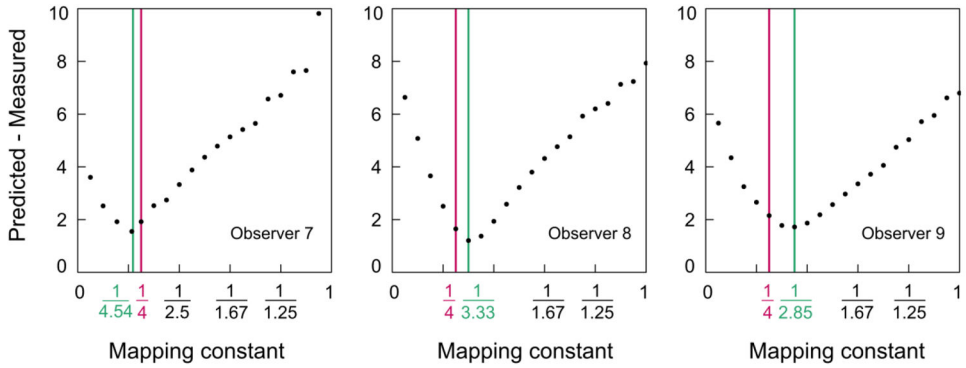

Figure 10.

Procedure for selecting the mapping rule. The dotted line traces the root mean square of difference between the measured and predicted transition ratios for different mapping constants in three observers. Every black dot corresponds to a mapping constant used in a separate simulation. In every panel, the red line marks the *standard* mapping constant 4^{-1} and the green line marks the *fitted* mapping constant. The fitted constants yield the values of transition ratios that are most similar to the measured ratios. The individual fitted constants are indicated in green below the abscissa.

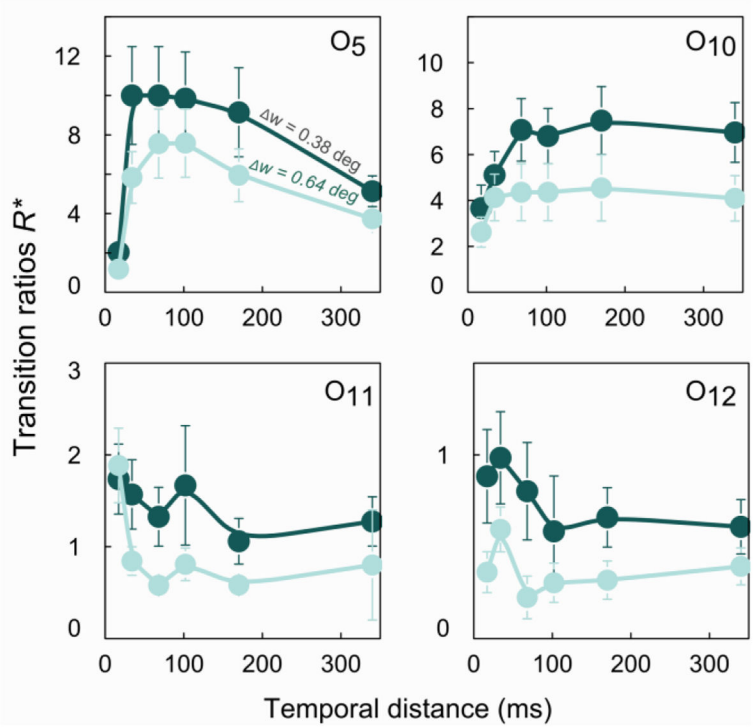

Figure 11.

Results of Experiment 4. Transition ratios for two within-dipole distances Δw are plotted as a function of temporal distance for four observers. The lines represent cubic spline fits to the transition ratios. Error bars represent ±1 SE. Observer 5 is one of the authors, who also participated in Experiment 2A.

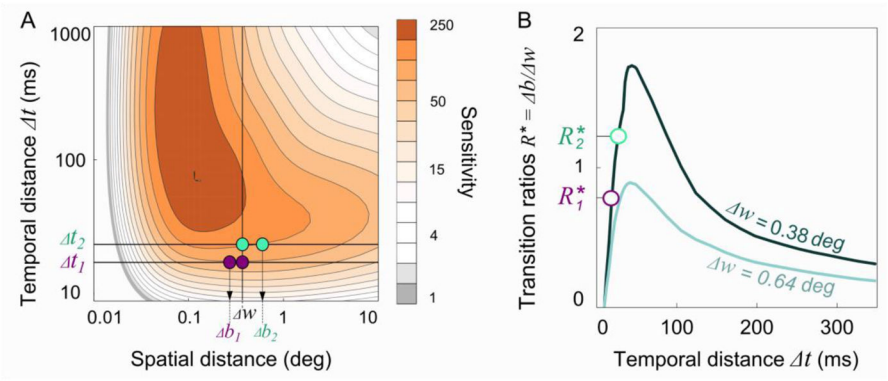

Figure 12.

Predictions for Experiment 4. (A) The Kelly function rendered as a graph of spatial and temporal distances between the dots, transformed as in (Kelly, 1979). Vertical lines indicate cuts of the sensitivity function at temporal distances Δt_1 and Δt_2. At Δt_1, points Δw and Δb_1 fall in the area of equivalent sensitivity, and at Δt_2, sensitivity is similar at points Δw and Δb_2. (B) The transition ratios predicted from the Kelly function for two within-dipole distances are plotted as a function of temporal distance. The unfilled circles mark the ratios of distances Δb and Δw indicated in panel (A).

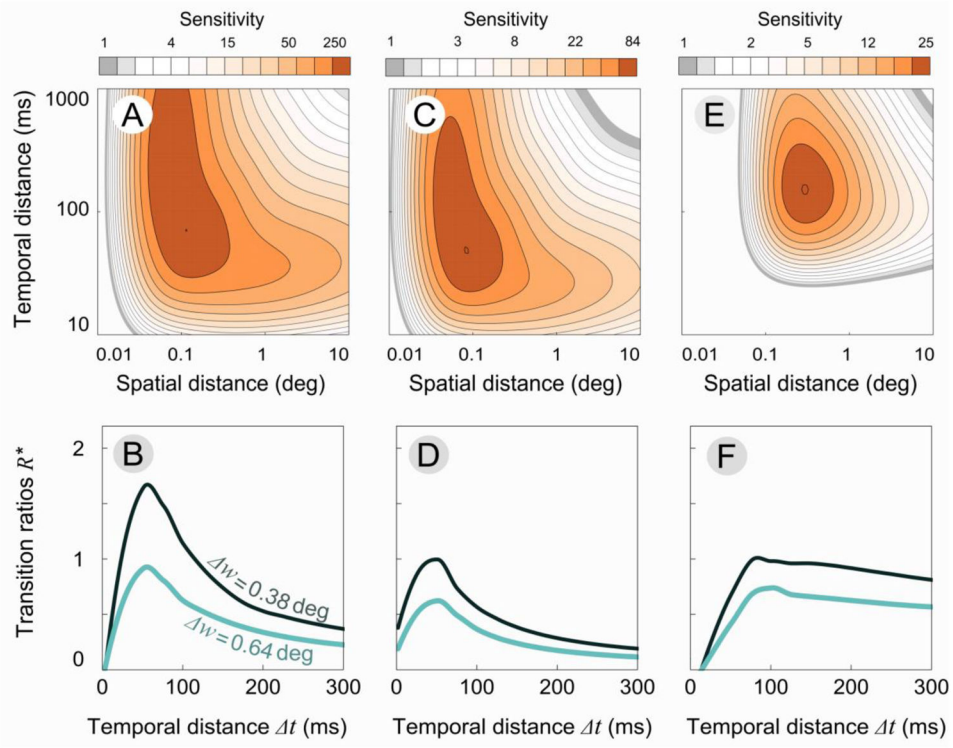

Figure 13.

Contrast sensitivity functions and predictions derived from them. (A), (C), (E) Contrast sensitivity functions are plotted as a function of spatial and temporal distances. Ordinate range is the same in all three plots. (B), (D), (F) Transition ratios predicted from sensitivity function are plotted as a function of temporal distance for two distances Δw. Ordinate range is the same in all three plots.

Table 1

Deviance table computed for two models fitted to log-odds as a function of the number of the dipoles for five within-dipole distances *Δw.* Model 1 fitted all data with a single logistic function. Model 2 fitted data with five psychometric functions corresponding to five distances *Δw.*

	Model 1 Degrees of freedom	**Model 2 Degrees of freedom**	**Model 1 Residual deviance**	**Model 2 Residual deviance**	**Δ *d*eviance**	**Chi-squared test of deviance, p**
Observer 1	80	72	92.4	49.58	42.82	9×10^{-7}
Observer 2	115	107	97.41	86.2	11.21	0.19
Observer 3	56	48	86.17	43.23	42.94	9×10^{-7}
Observer 4	46	38	92.87	38.66	54.21	6×10^{-9}

Table 2

Deviance table computed for two models fitted to log-odds as a function of the between-dipole distance *Δb* for five within-dipole distances *Δw.* Model 1 fitted all data with a single logistic function. Model 2 fitted data with five psychometric functions corresponding to five distances *Δw.*

	Model 1 Degrees of freedom	Model 2 Degrees of freedom	Model 1 Residual deviance	Model 2 Residual deviance	Δ *deviance*	Chi-squared test of deviance, p
Observer 1	80	72	81.08	46.25	34.83	2.8×10^{-5}
Observer 2	115	107	94.07	83.28	10.79	0.21
Observer 3	56	48	82.87	40.84	42.03	1.3×10^{-6}
Observer 4	46	38	90.55	52.67	37.88	6.3×10^{-6}

Table 3

Deviance table computed for two models fitted to log-odds as a function of the between-dipole distance *Δb* for five within-dipole distances *Δw.* Model 1 fitted all data with a single logistic function. Model 2 fitted data with five psychometric functions corresponding to five distances *Δw.*

	Model 1 Degrees of freedom	**Model 2 Degrees of freedom**	**Model 1 Residual deviance**	**Model 2 Residual deviance**	**Δ *deviance***	**Chi-squared test of deviance, p**
Observer 5	233	225	225.38	169.67	55.71	3.2×10^{-9}
Observer 6	106	98	109.21	69.5	39.71	3.6×10^{-6}